Electrodialysis for concentrating cobalt, chromium, manganese, and magnesium from a synthetic solution based on a nickel laterite processing route

*G.C. Feijoo [1]; K.S. Barros [1,2,3]; T. Scarazzato [3]; D.C.R. Espinosa [1].

[1] Department of Chemical Engineering, University of São Paulo (USP). Address: Av. Professor Lineu Prestes, 580, Bloco 18 – Conjunto das Químicas, 05434-070. São Paulo – SP. Brazil.

[2] IEC Group, ISIRYM, Universitat Politècnica de València (UPV) – Spain. Address: Camí de Vera s/n, 46022, P.O. Box 22012, València E-46071, Spain.

[3] Department of Materials Engineering, Federal University of Rio Grande do Sul (UFRGS). Address: Av. Bento Gonçalves, 9500, 91501-970, Porto Alegre - RS, Brazil.

*Corresponding author: gustavofeijoo@alumni.usp.br

Abstract: Due to environmental and human health concerns, the need for cleaner techniques able to extract and recover metals from mining process solutions has been increasing. In this work, the use of electrodialysis for recovering cobalt, magnesium, manganese, and chromium ions from an acid multicomponent solution generated in the nickel laterite processing was evaluated. Values of percent extraction above 98% were obtained for Co^{2+}, Mn^{2+}, and Mg^{2+} ions. For Cr^{3+}, the greatest percent extraction obtained was 83%. The results of percent concentration of the species showed the same trend: for Cr^{3+} ions, it was significantly lower than the others. Such difference in the transport of the metals through the membranes may have occurred due to the lower molar concentration, lower diffusion coefficient, and greater Stokes radius of chromium ions. Thus, the transfer of Cr^{3+} was hindered by the presence of other cationic species. This was also evidenced by the results of current efficiency and energy consumption associated with each species in solution. Lastly, the results of solution pH throughout the experiments and the final condition of the membranes, which were analyzed by SEM/EDS, indicated that the water dissociation phenomenon occurred at their surfaces.

Keywords: Electrodialysis; ion-exchange membrane; hydrometallurgy; metal recovery; nickel ore.

1. Introduction

In recent decades, the exploration of nickel from laterite ores has shown a strong increase due to the nickel depletion in the sulfide deposits. Besides, the obtaining of cobalt as a secondary source is favored in the nickel laterite processing due to its greater content compared to sulfide ores and because cobalt is mostly located on the laterite ore surface, which facilitates its extraction. This is advantageous since cobalt is a valuable metal traditionally obtained from nickel mining [1,2].

The nickel laterite ore processing is conventionally conducted via a hydrometallurgical route [1,3,4], which may involve high-pressure acidic leach (*HPAL process*) or Caron process, though atmospheric leaching and heap leaching may represent lower cost alternatives. After leaching, separation and purification steps are usually carried out by means of precipitation, solvent extraction and electrowinning. During the nickel refining stage, solvent extraction is one of the few viable commercial techniques for separating nickel and cobalt present in the leachate because these metals present similar properties, such as density and standard reduction potential [5,6]. However, this technique presents risks for the environment and human health, mainly due to the storage of great amounts of flammable/toxic organic compounds, increasing its investment and operating costs [7–9]. Hence, the search for alternative or complementary methods for extracting and refining metals from solutions generated in the solvent extraction stage has been encouraged to overcome the above-mentioned limitations.

In the last years, some routes involving multiple stages of solvent extraction have been proposed [5,10,11], allowing an effective recovery of nickel. However, the extract solutions generated in each stage may contain several other metals of economic interest, as recently showed by Aliprandini et al. [10,12]. The authors proposed a feasible route using solvent extraction to obtain nickel from the sulfuric acid leaching liquor; in the last stage of the process, two solutions were generated: a Ni-rich raffinate and an organic phase containing significant amounts of magnesium, cobalt, manganese, and chromium. Among these metals, magnesium and cobalt are elements of great economic relevance and have been considered as critical metals; they are mostly used in emerging technologies but face the threat of an abrupt interruption of their supply. Therefore, the recovery of such metals is of great interest. In this case, electrodialysis may be used as a method to concentrate and recover these valuable metals from the extract solution of the

solvent extraction process, improving the nickel processing and favoring the circular economy.

Electrodialysis (ED) is an environmentally friendly technique that allows the separation of ionic species through ion-selective membranes that are arranged in parallel between two electrodes positioned at the extremities of the system. Under the application of an electric field, cationic species migrate towards the cathode, whereas anionic species migrate towards the anode. Theoretically, cation-exchange membranes (CEM) allow only the passage of cations, whereas anion-exchange membranes (AEM) allow only the passage of anions. Thus, from an initial electrolytic solution, two types of solutions are generated: one more concentrated and another more diluted than the initial one [13,14]. In recent years, electrodialysis has been often used as a separation technique in several industrial fields, because it allows the recovery of valuable ionic species, it does not require addition of further chemicals, it is operated at ambient temperature and without pressurization, and its impact on the environment is minimal if compared to other techniques [15–17]. A schematic drawing of a typical electrodialysis system is shown in Figure 1.

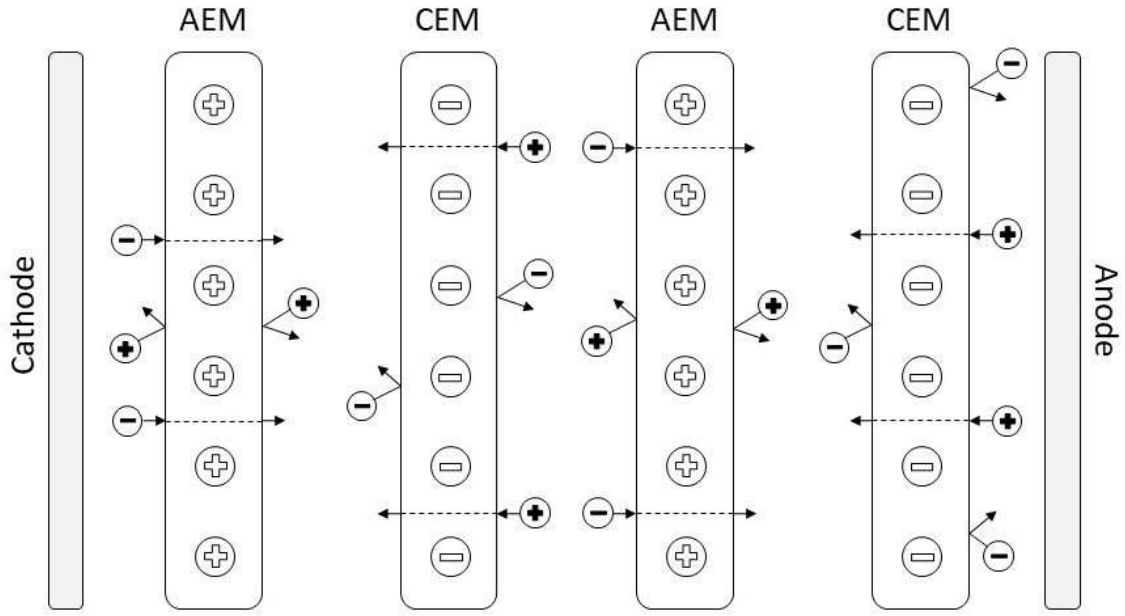

Figure 1 - Typical electrodialysis system with cation-exchange membranes (CEM) and anion-exchange membranes (AEM).

It is important to avoid operating the electrodialysis system under conditions of intense concentration polarization to guarantee its viability. Concentration polarization

occurs if the applied current density is equal or greater than the limiting current density (i_{lim}) of the membrane/electrolyte system [18,19]. This undesirable phenomenon may lead to the deposition of organic (fouling) and inorganic substances (scaling) at the membrane surface, increasing the membrane resistance and energy consumption of the process [20,21]. Thus, before operating electrodialysis, the limiting current density must be determined by using one of the widely known techniques for this purpose, which is the construction of curves of electric current versus membrane voltage, also known as current-voltage curves (CVC) [22,23].

Considering the need to improve the nickel laterite processing and the advantages of using electrodialysis for treating electrolytes, the present work aims at evaluating the ED application as a complementary method in the solvent extraction stage of nickel laterite processing. The solution treated herein was based on the extract phase obtained by Aliprandini et al. [10,12], which contained Co^{2+}, Mn^{2+}, Mg^{2+}, Cr^{3+}, H^{+} and SO_4^{2-} species. The electrodialysis was conducted in batch mode and its performance was evaluated in function of percent extraction and percent concentration of the species, in addition to the pH and conductivity of the solutions throughout the test. Current efficiency and energy consumption associated with each ionic species at several moments of the experiment were also determined. The condition of the membranes after the electrodialytic process was evaluated by means of SEM/EDS.

2. Experimental

2.1. Electrodialysis bench system configuration

A laboratory-scale electrodialysis stack was used to treat the synthetic sulfate solution simulating an acidic waste from the nickel laterite processing. The experiments were carried out in a six-compartment cell, each compartment presenting dimensions of (40x40x10) mm, made of acrylic, and connected to three 0.5 L reservoirs. The intermembrane distance between the compartments was 10 mm, for evaluating the ion transfer in a less turbulent system. The stack configuration was electrode/cathode-AEM-CEM-AEM-CEM-AEM-electrode/anode. Commercial heterogeneous ion-exchange membranes (Hangzhou Iontech Environmental Technology Co., Ltd., China) were positioned between the compartments. The cation-exchange membranes (IONSEP-HC-

C, also known as HDX100) have sulfonic acid as fixed groups attached to the membrane matrix, whereas the anion-exchange membranes (IONSEP-HC-A, also known as HDX200) present quaternary amine groups. The main characteristics of both membranes are shown in Table 1. The electrodes positioned at the side compartments of the system were made of titanium coated with titanium and ruthenium oxides ($70RuO_2/30TiO_2$). Both electrodes and the membranes had an effective area of 16 cm^2. A power supply was connected to the electrodes.

Table 1 - Main characteristics of HDX100 and HDX200 membranes provided by the supplier [18].

Parameter	HDX100	HDX200	Unit
Ion group attached	- SO_3^-	- NR_3^+	-
Water content	35-50	30-45	%
Ion exchange capacity	≥ 2.0	≥ 1.8	$mol \cdot kg^{-1}$ (dry)
Surface resistance (measured in 0.1 $mol \cdot L^{-1}$ NaCl)	≤ 20	≤ 20	$ohm \cdot cm^2$
Permeselectivity (0.1 $mol \cdot L^{-1}$ KCl/0.2 $mol \cdot L^{-1}$ KCl)	≥ 90	≥ 89	%
Burst strengh	≥ 06	≥ 0.6	MPa
Dimensional change rate	≤ 2	≤ 2	%
Water permeability	≤ 0.1 (< 0.2 MPa)	≤ 0.2 (< 0.035 MPa)	$mL \cdot h \cdot cm^{-2}$

The tests were performed in galvanostatic mode to evaluate the ion transfer in distinct conditions, including in the overlimiting current region. The current density applied to the system was 80% of the initial limiting current density of the membranes/electrolyte system, which was determined by constructing current-voltage curves of both membranes, as described in references [14,24]. For this, platinum wires were placed at the interfaces of the cation- and anion-exchange membranes facing the diluted and concentrated solutions. Platinum wires were connected to voltmeters for measuring the potential drop near the surface of both membranes under increasing applied current densities.

Electro-pumps were used to allow the circulation of the solutions (80 $L.h^{-1}$). A schematic representation of the electrodialysis system is shown in Figure 2, whereas the real ED system used is shown in Figure 3.

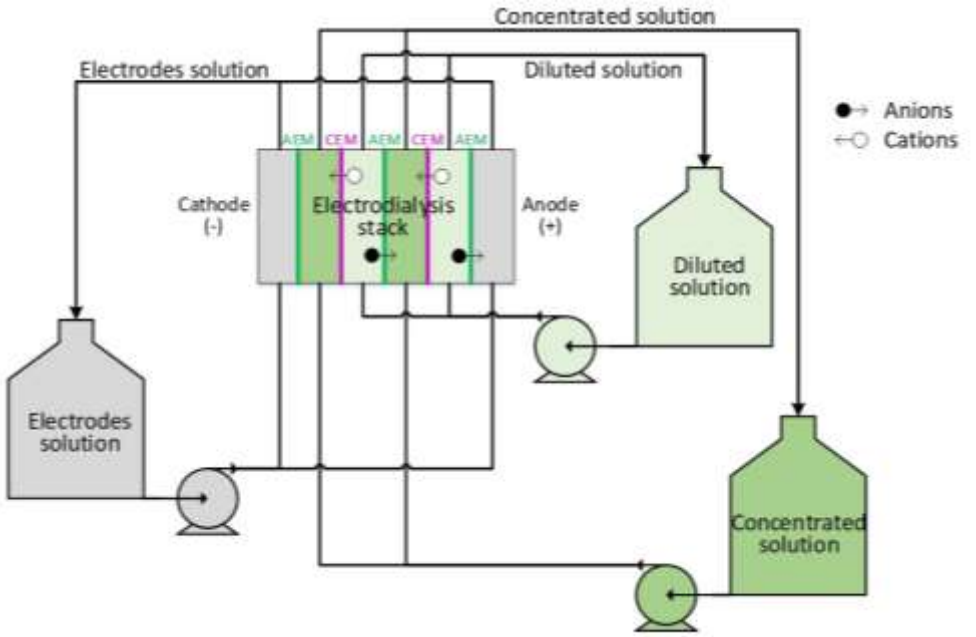

Figure 2 - Schematic representation of the ED system used.

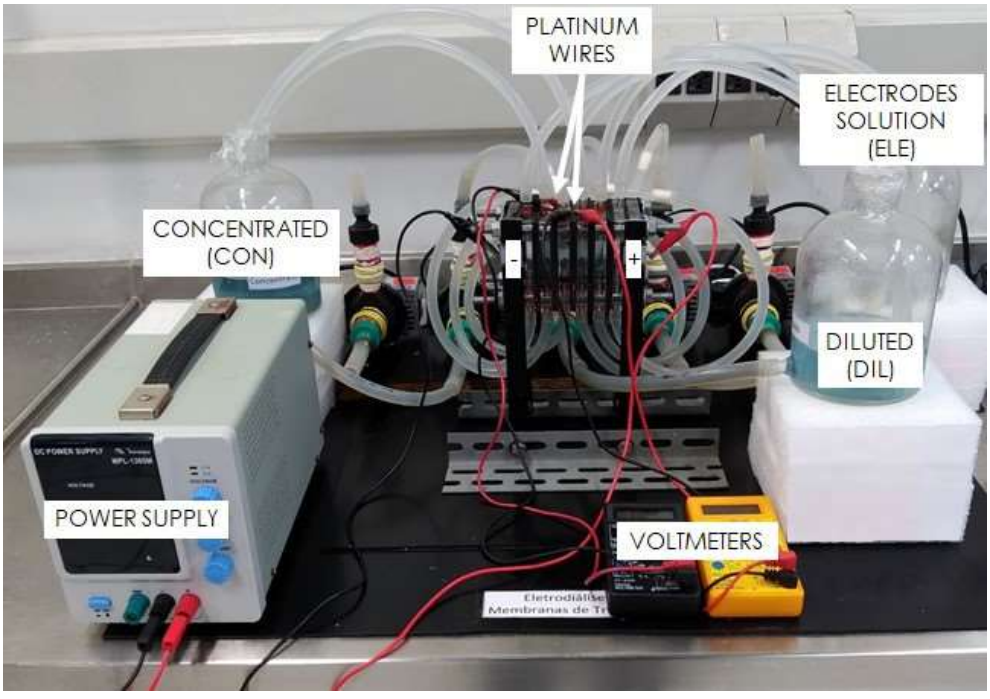

Figure 3 - Electrodialysis system with the dilute (DIL), concentrate (CON), and electrodes (ELE) compartments, the power supply, and the voltmeters.

149 2.2. Experimental procedure

150 Three reservoirs were used to feed the six-compartment cell. The solutions were
151 pumped independently from the reservoirs to the stack (compartments), forming a closed
152 system for each solution. Thus, the objective was to obtain two solutions: a concentrated
153 one containing the ions of interest and another more diluted than the initial solution. The
154 reservoir connected to the two compartments where the solution would be desalted was
155 labeled diluted solution (DIL). The dissociated ions in the DIL solution would migrate to
156 the adjacent compartments that were labeled concentrated solution (CON). The electrode
157 compartments (ELE) were filled with a salt solution to maintain the electrical
158 conductivity of the system. The experiment was performed in duplicate and the relative
159 errors between the concentration values were below 5%.

160 The pH and electrical conductivity of all reservoirs were monitored throughout the
161 experiment. When the electrical conductivity of the diluted solution decreased down to
162 0.8 $mS.cm^{-1}$, the diluted solution was replaced with a new working solution, and the
163 experiment was reconducted. Each renewal of the diluted solution was named “batch”.
164 At the end of each batch, the diluted solution was forwarded to chemical analyses,
165 whereas the solution from the concentrate compartment was analyzed only at the end of
166 the experiment, after all batches. The performance of electrodialysis was assessed in
167 function of percent extractions and percent concentrations of the main ionic species in
168 solution (Co^{2+}, Mn^{2+}, Mg^{2+}, Cr^{3+}, and SO_4^{2-}), as shown in Equation (1) and Equation (2),
169 respectively. In the equations, C_0^j and C_t^j are the concentration of an ion j in the initial
170 state and at a given time, respectively. As percent extractions were calculated with data
171 on the diluted solutions after each batch, the values obtained were lower than 100%. For
172 percent concentrations, the values obtained were greater than 100% because they were
173 determined using data on the concentrate compartment after all batches, which means
174 they were accumulative.

175

$$Percent\ extraction\ (\%) = \left(1 - \frac{C_t^j}{C_0^j}\right).100 \qquad (1)$$

176

$$Percent\ concentration\ (\%) = \left(\frac{C_t^j}{C_0^j} - 1\right).100 \quad (2)$$

177

178 Another electrodialysis test was conducted in a single batch using the same working
179 solution, electrode solution, and ED apparatus described in section 2.1, to determine the
180 energy consumption and the current efficiency of the main ionic species. This test was
181 conducted until the conductivity of the diluted compartment reached 0.8 $mS.cm^{-1}$. 10 mL
182 samples were collected every 4 h from the solutions of the DIL and CON compartments
183 and forwarded to chemical analyses; with data of pH and chemical composition of the
184 aliquots, speciation diagrams were constructed with the aid of Hydra-Medusa software
185 [25] for each sample. Then, the concentrations of the main ionic species present in the
186 aliquots were determined. With data on the ionic species at different moments, Equation
187 (3) and Equation (4) were used to determine the current efficiency and the energy
188 consumption, respectively, associated with each ionic species. In the equations, η_j is the
189 current efficiency of an ion *j*, z is its charge, *F* is the Faraday constant, n_j is the number
190 of mols of the ion *j* transferred from the diluted to the concentrated compartment, *N* is the
191 number of cell pairs, *I* is the electric current, *t* is time, *U* is the electric potential and m_j
192 is the mass of the transported species *j* from the diluted to the concentrated compartment.

$$\eta_j = \frac{z.F.n_j}{N.\sum_{t=0}^{t} I.\Delta t} \quad (3)$$

193

$$E_j = \frac{\sum_{t=0}^{t} U_{\Delta t}.I_{\Delta t}.\Delta t}{m_j} \quad (4)$$

194

195 2.3. Working solutions

196 The synthetic solution to be treated, or working solution, was prepared based on the
197 leaching liquor from the nickel laterite processing obtained by Aliprandini et al. [10,12].
198 The authors reported the composition of the final solutions obtained by a multiple-stage
199 solvent extraction route. The final raffinate obtained by the authors presented 2.52 $g.L^{-1}$

of nickel. The organic phase (extract) contained 0.050 $g.L^{-1}$ of cobalt, 0.152 $g.L^{-1}$ of chromium, 6.160 $g.L^{-1}$ of magnesium, and 0.360 $g.L^{-1}$ of manganese. Hence, the synthetic solution treated herein, by electrodialysis, simulated the sulfuric stripping solution from the last liquid-liquid extraction step. It was assumed that all the metals were reextracted from the organic phase.

The working solution was prepared with $CoSO_4.7H_2O$, $MnSO_4.H_2O$, $MgSO_4.7H_2O$, $Cr_2(SO_4)_3$, and distilled water. The pH of the working solution was adjusted to 1.8, which is the pH value of the stripping solutions in industries [11]. The electrical conductivity of the working solution was 28 $mS.cm^{-1}$. The solution of the electrodes compartment was prepared with sodium sulfate (Na_2SO_4) and distilled water. The initial composition of the working and electrodes solutions is shown in Table 2.

Table 2 - Initial composition of the working and electrodes solutions.

	Ion concentration ($mg.L^{-1}$)		
	ELE	DIL	CON
Co^{2+}	-	41	41
Mg^{2+}	-	4735	4735
Mn^{2+}	-	308	308
Cr^{3+}	-	183	183
Na^{+}	9700	-	-
SO_4^{2-}	23000	27100	27100
λ ($mS.cm^{-1}$)	40	28	28
pH	1.8	1.8	1.8

2.4. Analytical methods

The analyses of cationic species were performed by atomic emission spectrometry by coupled plasma (ICP-OES), model Agilent 710. The analyses of sulfate (SO_4^{2-}) were carried out by ion chromatography (Metrohm 850 Professional IC AnCat-MCS and 858

Professional Sample Processor). The pH of the solutions was measured with a Lovibond Sensodirect 150 meter, and the electrical conductivity with a Tecnal model meter Tec-4MP.

2.5. SEM/EDS analysis

After the electrodialysis experiments, the membranes from the diluted compartment were rinsed with distilled water, dried for 24h at 60°C in vacuum oven, and their surfaces were analyzed using a Scanning Electron Microscope (Phenom ProX) and a Back Scattered Electron Detector (BSE), equipped with Energy-Dispersive X-ray Spectroscopy (SEM/EDS) at 5 kV of accelerating voltage. The SEM/EDS analyses were carried out for at least three regions of each membrane to evaluate their overall physical structure and the occurrence of scaling.

3. Results and Discussion

3.1. Evaluation of ionic species in the initial working solution and the pH throughout the electrodialysis test

A speciation diagram was constructed with the aid of Hydra-Medusa software [25] using the composition of the initial working solution (Table 2), for visualizing the ionic species present in the solution as a function of pH. The speciation diagram is shown in Figure 4.

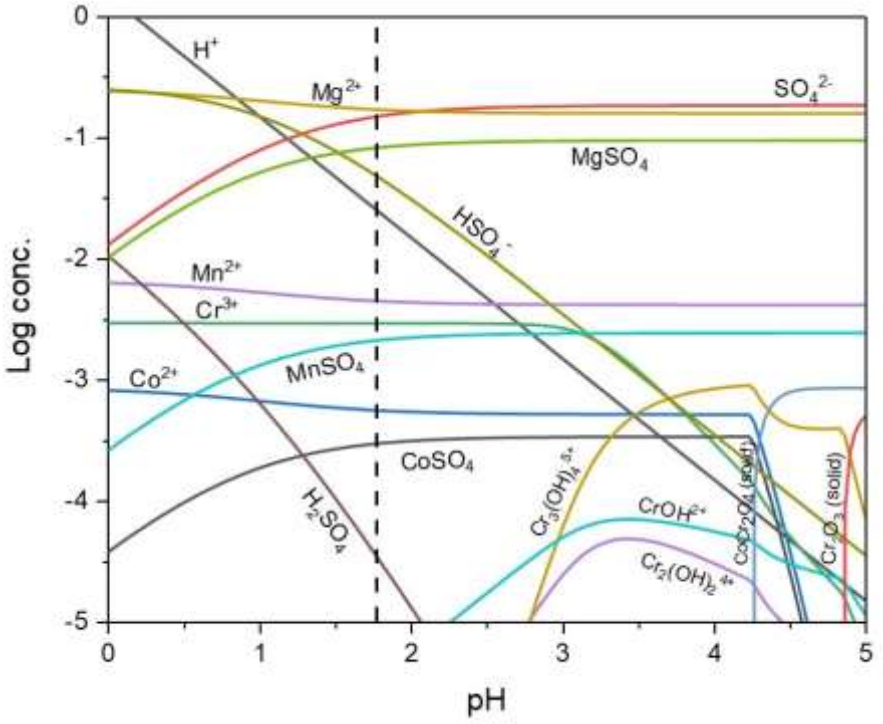

Figure 4 - Speciation diagram constructed with the composition of the initial working solution. The vertical/dashed line indicates pH 1.8.

With composition data of the main ionic species in the working solution shown in Figure 4 (at pH 1.8), the anionic and cationic equivalent charges (Q_{eq}) were determined. This property was calculated by the product of the concentration (C_j) of the anionic or cationic species and their charge (z_i), as expressed by Equation (5) [26,27]. For the anionic and cationic species, the obtained equivalent charge was $3.5x10^{-1}$ Eq.L^{-1} and $3.6x10^{-1}$ Eq.L^{-1}, respectively, which is in accordance with the electroneutrality requirements.

$$Q_{eq} = \sum |z_j| C_j \quad (5)$$

Figure 4 also indicates that the metals were present in the free form mainly at pH below 4. Solid species, such as $CoCr_2O_4$ and Cr_2O_3, begin to be formed above this value, which could affect the electrodialysis performance. For this reason, the pH of the solutions was monitored during the ED test.

The pH profile in each compartment throughout the electrodialysis is shown in Figure 5. The pH of the electrode solution showed a lower variation over the test compared to the other solutions, remaining virtually constant. The pH in the diluted compartment increased up to 2.7, whereas in the concentrate compartment it decreased down to 1.5.

This may be explained by the intense transport of H^+ ions through the CEM since the working solution was acidic and protons are transferred intensively by the Grotthuss mechanism [28]. Besides, H^+ ions present a lower Stokes radius and greater diffusion coefficient than the other species, intensifying their migration. Data on the diffusion coefficient and Stokes radius of the main ions present in the solutions are shown in Table S1 of the Supplementary Material [29,30].

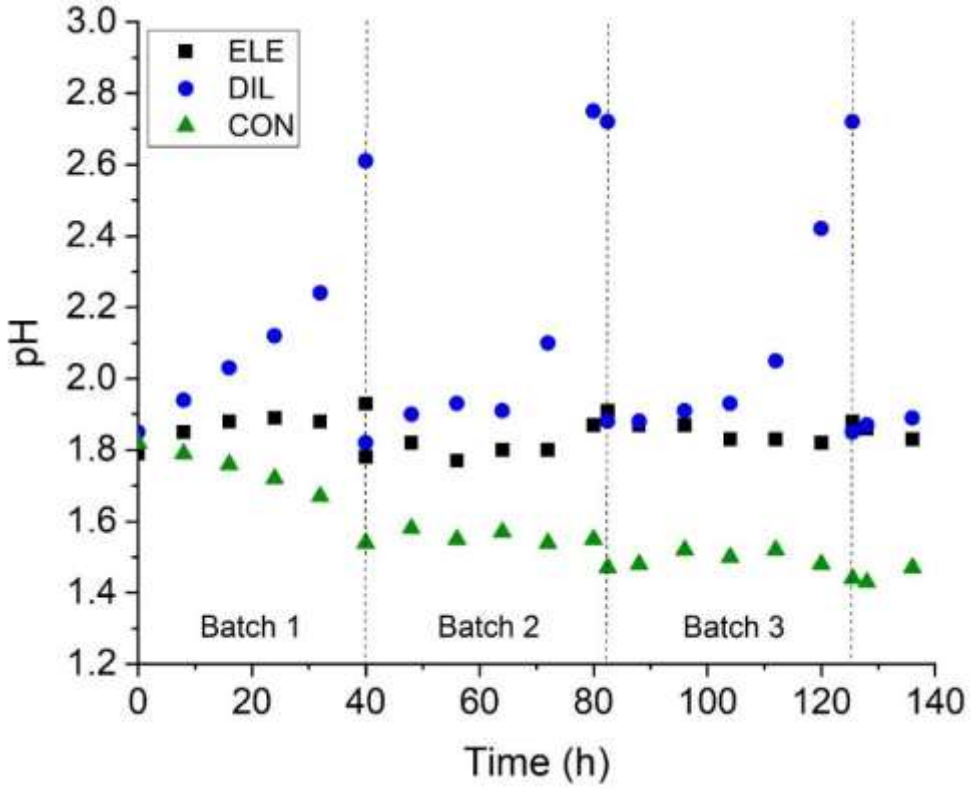

Figure 5 - pH profile of solutions in the ELE, DIL, and CON compartments throughout the electrodialysis test. Vertical lines delimit each batch.

Note that as the test was conducted and the concentration of the diluted solution decreased in all batches, a sharp increase in its pH was verified, mainly during the last 10 hours of each batch. This may have occurred due to the lower competition between protons and other ions to cross the CEM, which enhanced its migration to the concentrated compartment. Another hypothesis is the occurrence of intense water dissociation at the diluted side of the cation-exchange membrane because as the concentration of the diluted solution decreased, the limiting current density of the membrane/electrolyte system also decreased [21,31]. The current density applied to the ED unit was constant over the test. Hence, the membrane/electrolyte system operated at overlimiting conditions during the last hours of each batch., which means that an intense concentration polarization occurred

at the membranes. This may have led to water dissociation at the cation-exchange membranes, which generated H^+ and OH^- ions [32]. The intense transport of H^+ ions through the CEM and the accumulation of OH^- ions on its diluted side may have been responsible for the pH increase of the diluted solution. Water dissociation may also have occurred at the surface of the AEM, as will be shown in the evaluation of current efficiency (Section 3.3). The hypothesis of the operation under overlimiting current regimes can be confirmed by evaluating the total potential of the electrodialysis stack throughout the test, which is shown in Figure 6. Note that the total stack potential remained below 10 V until approximately the first 30 h of each cycle. In the last 10 h, the potential reached the maximum limit of the power supply (33 V); at that moment, the scarcity of ions in the diluted solution promoted an increase in its resistivity, and consequently, the total potential. When the diluted solution from the DIL compartment was changed to start a new batch, the total potential returned to values below 10 V. As shown in Figure 5, this behavior was similar to the pH profile of the diluted compartment.

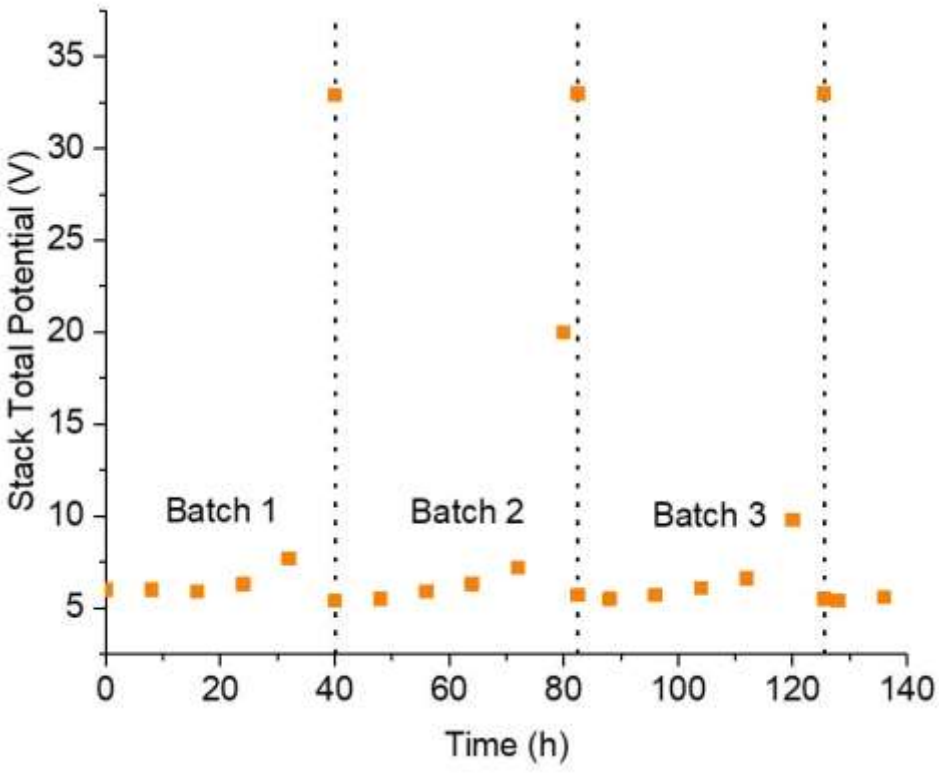

Figure 6 - Stack total potential during the assay. The vertical lines delimit the batches.

3.2 Electrical conductivity, percent extraction, and percent concentration

The limiting current density of the membranes/electrolyte system was determined by constructing current-voltage curves for the CEM and AEM; the standard error between the duplicate curves was between 1-3%. The i_{lim} obtained for the anion- and the cation-exchange membrane was 9.2 $mA.cm^{-2}$ and 8.3 $mA.cm^{-2}$, respectively. Hence, the current density initially applied to the electrodialysis test was 80% of the limiting current density of the CEM (6.6 $mA.cm^{-2}$) since its value was lower than the i_{lim} of the AEM.

The electrodialysis test was performed over 136h because, after this period, the electrical conductivity of the CON solution remained constant due to diffusion limitations. Three batches were completed, and the duration of each one increased throughout the test, which may be explained by the increase of the concentration gradient between the DIL and CON solutions.

The conductivity variation throughout the electrodialysis test is presented in Figure 7. As verified, the final conductivity of the DIL solution was 0.8 $mS.cm^{-1}$ at the end of all batches. In the concentrated reservoir, the conductivity reached 61.3 $mS.cm^{-1}$ at the end of the experiment, which means the conductivity increased by 119% after 136h of ED. This result can be associated with the ions recovery since the electrical conductivity is proportional to the concentration of ions in the solution. After 125h, no remarkable increase in the conductivity of the CON solution occurred. This may have occurred after the third batch due to the considerable concentration gradient between the compartments and the tendency of diffusion of ions from the CON to the DIL solution.

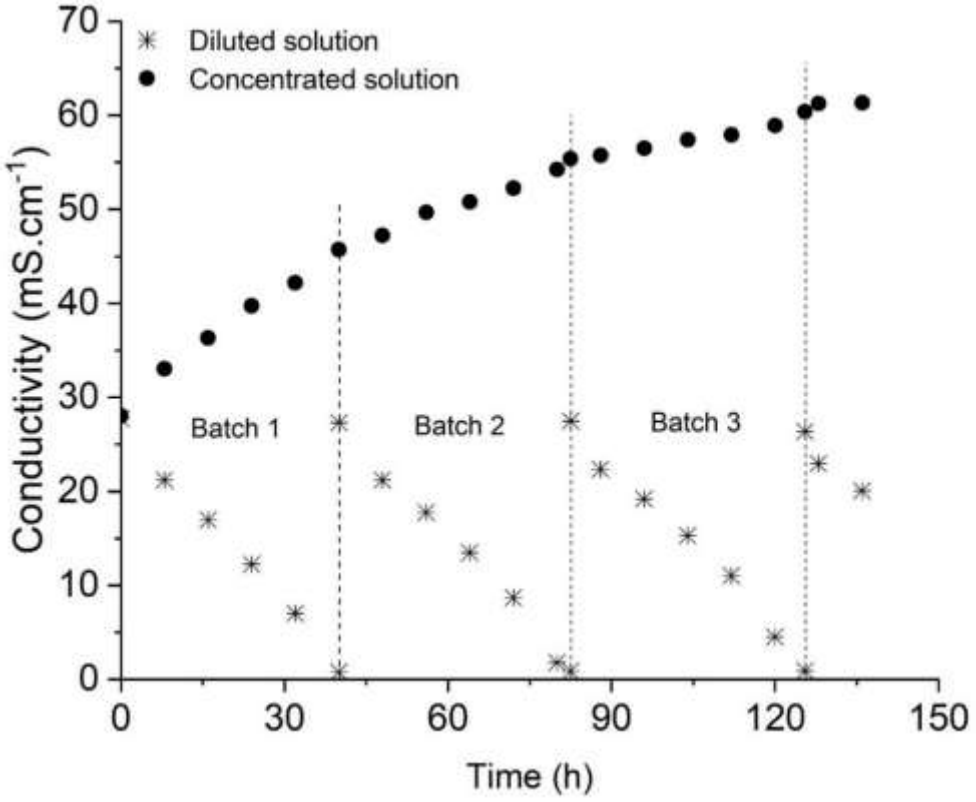

Figure 7 - Behavior of the electrical conductivity during electrodialysis. Vertical lines delimit each batch.

Aliquots were collected from the DIL compartment at the end of each batch to be analyzed by ICP-OES and ion chromatography, whereas the solution in the CON compartment was analyzed only at the end of the electrodialysis test. The results are presented in Table S2 (Supplementary Material). With concentration data of the main ions present in the diluted solution after each batch, the percent extractions of each ion were determined by Equation (1), and the results are shown in Figure 8. With data of concentrations of ions in the concentrated solution at the end of the electrodialysis test, the percent concentrations were determined by Equation (2), as shown in Figure 9.

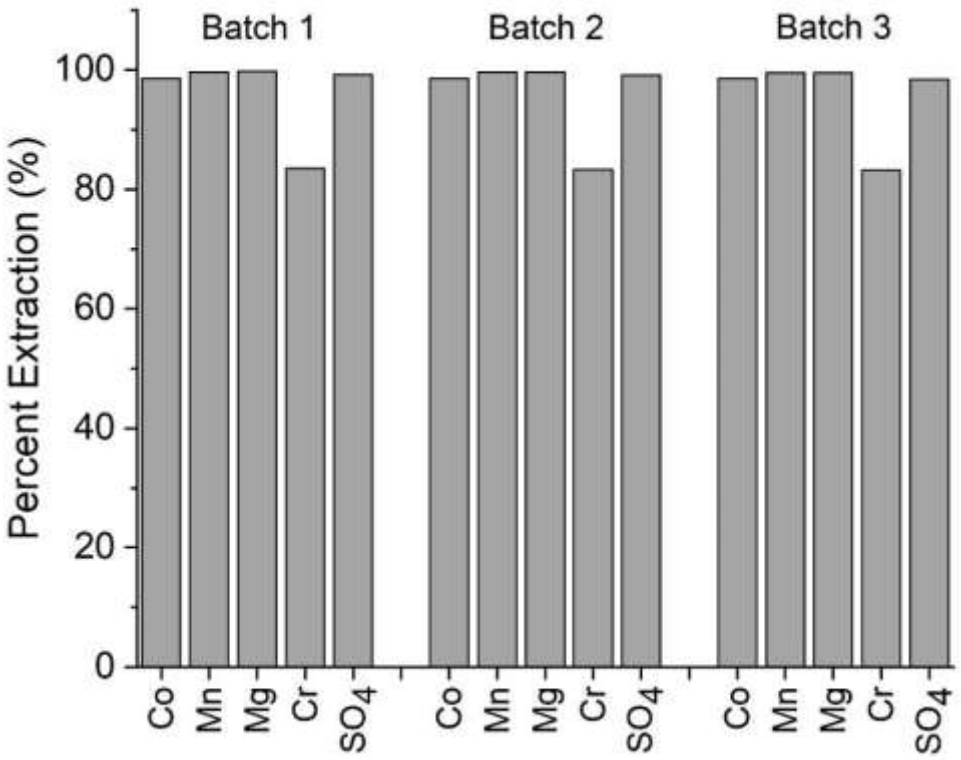

Figure 8 - Percent extraction for the main ionic species in the solution after each electrodialysis batch.

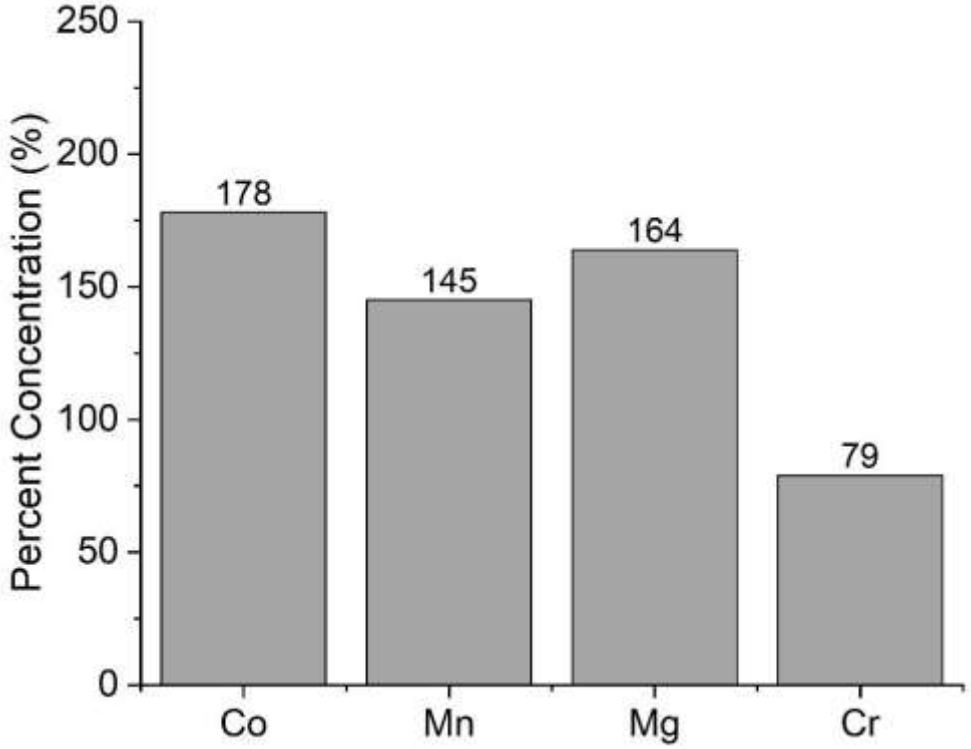

Figure 9 - Percent concentration for the main ionic species in the solution at the end of the electrodialysis test.

According to Figure 8, the values of percent extraction of Co^{2+}, Mn^{2+}, Mg^{2+}, and SO_4^{2-} were similar, reaching values above 98% after all batches. Conversely, the percent extraction of Cr^{3+} ions showed lower values after all batches, reaching values up to 83%. As Cr^{3+} ions have the greatest charge if compared to the other metals in solution, a greater migration of this ion was expected, due to the higher attraction between ions and fixed charges of the CEM [33–35]. The opposite behavior may have occurred due to the size of Cr^{3+} ions; they have the greatest Stokes radius among the metal ions in the solution and, consequently, the lowest diffusion coefficient (Table S1 – Supplementary Material). Besides, it is known that the transfer of trivalent ions through ion-exchange membranes is a complex phenomenon because their high charge density leads to an important hydration shell [36]. This may also be related to the selectivity of the CEM; Dalla Costa et al. [37] showed that membranes with sulfonic acid present lower affinity to trivalent cations, such as chromium (III) and iron (III), than to other ions. Hence, the HDX100 membrane may be more selective to the other ions in solutions than to Cr^{3+}.

According to Figure 9, the values of percent concentration obtained for the cations were 178% for Co^{2+}, 145% for Mn^{2+}, 164% for Mg^{2+}, and 79% for Cr^{3+}. The low percent concentration obtained for Cr^{3+} ions can also be explained by its lower diffusion coefficient and concentration than the other metals, besides the selectivity of the membrane to bivalent ions. At the end of electrodialysis, sodium ions were present in the concentrated solution. As the initial working solution did not contain sodium ions (Table 2), their presence in the concentrated compartment may be explained by the migration of these ions from the electrode compartment towards the concentrated one. Thus, anionic species containing sodium, probably in the form of $NaSO_4^-$, present in the cathode crossed the AEM towards the anode and accumulated in the concentrated solution (see Figure 2). Sodium was not considered in the evaluations of percent extraction and percent concentration because it was not present in the initial working solution.

Moreover, it can be noted in Figure 8 and Figure 9 that the percent extraction of the metal ions does not correspond to their percent concentrations. Two hypotheses could be established: (1) a portion of metal ions may have been adsorbed in the membranes, or (2) a significant transfer of solvent (water) occurred through the membranes. For evaluating the first hypothesis, the membranes were analyzed after electrodialysis.

Figure S1 (see the Supplementary Material) shows the visual aspect of the membranes from all the compartments before and after electrodialysis. CAT, CCAT, CANO, and ANO refer to the membranes facing the cathode, the concentrated solution

at the cathodic side, the concentrated solution at the anodic side, and anode, respectively. As verified, the images suggest the formation of precipitate inside the membranes, especially the AEM, which was confirmed by the SEM/EDS analysis shown in Figure 10.

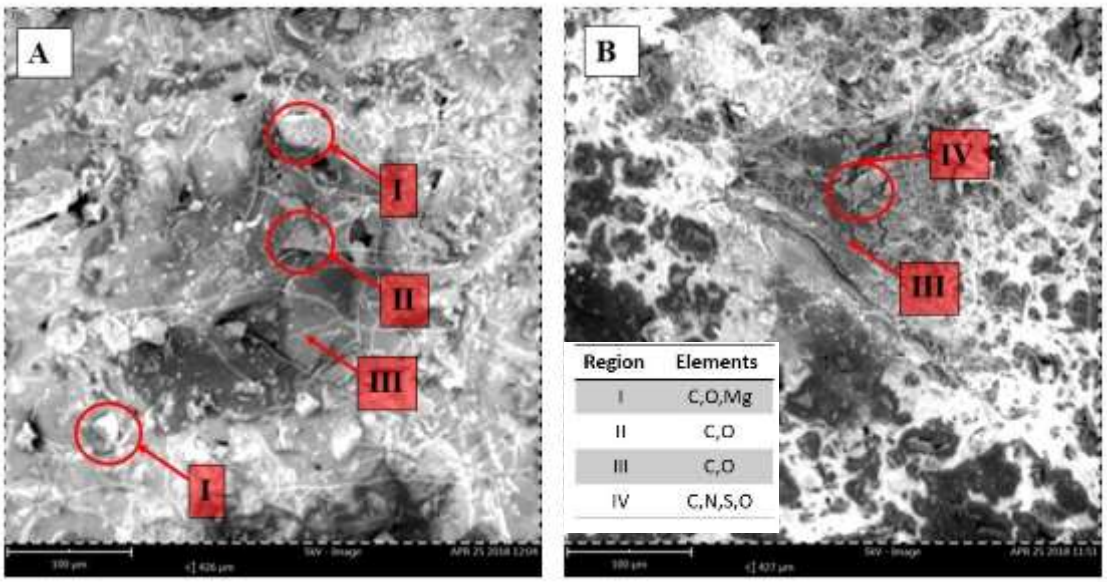

Figure 10. Backscattered electron images obtained by scanning electron microscopy for the (A) CEM and (B) AEM after electrodialysis: (I) indicates the spots at which the presence of magnesium was detected by EDS, (II) and (IV) are ion-exchange particles and (III) reinforcement fibers.

According to Figure 10, the SEM images did not indicate considerable damages in the structure of the membranes after electrodialysis. The presence of nitrogen in region IV of the AEM may be explained by the amine groups of the ion-exchange particles. The presence of Mg at the CEM (region I) may be explained by the occurrence of water dissociation at the membrane surface, as mentioned in Section 3.1. These results are in accordance with the pH evaluation shown in Figure 5.

Despite the presence of magnesium at the CEM, the disproportionate relation between the percent extraction and percent concentration of ions is not explained (Figure 8 and Figure 9). Thus, a hypothesis regarding the solvent (water) transfer through the membranes was also considered. It is well known that ion-exchange membranes used in electrodialysis are not perfectly permselective, allowing the transport of solvent mainly by osmosis and electro-osmosis. The osmosis mechanism results from osmotic pressure created by the difference of ion concentration between diluted and concentrated solutions.

The electro-osmosis results from the ion solvation when transported through the membranes [38–40]. As verified in Figure 7, the difference of electrical conductivity between the diluted and concentrated compartments reached approximately 50 mS/cm^{-1}, which indicates a large difference in ion concentration, and consequently, a high osmotic pressure. Besides, electro-osmotic effects are time-dependent [41], which means that even if the rate of water transport is low, electro-osmosis may play an important role in long-term assays. In fact, at the end of the test, a higher volume in the concentrated reservoir was noted, compared to the diluted and electrodes ones.

3.3 Current efficiency and energy consumption

Another electrodialysis test was conducted in a single batch using the same solutions and ED apparatus described in Section 2.1. This one-batch test was conducted for 40 hours and aliquots were collected every 4h to be forwarded to chemical analysis, i.e., after 4h, 8h, 12h, 16h, 20h, 24h, 28h, 32h, 36h, and 40h of electrodialysis. This experiment was performed to evaluate the current efficiency, energy consumption, and percent extractions of the main ionic species present in the DIL solution in function of time. Figure 11 shows the results of percent extractions throughout the test.

The percent extraction of Co^{2+}, Mn^{2+}, Mg^{2+}, and SO_4^{2-} showed a behavior virtually linear throughout the test and reached values greater than 95% (Figure 11). For Cr^{3+} ions, the percent extraction remained below 20% until 30h, and then it showed a sharp increase, reaching 85%. This may have occurred due to the lower selectivity of the cation-exchange membrane to Cr^{3+} ions than the other metals, as already mentioned. In electrodialysis, the migration of ions towards the electrodes occurs since the system seeks the electroneutrality condition. Firstly, ions presenting small size, high concentration, and high mobility/diffusion coefficient are preferentially transferred through the membranes.

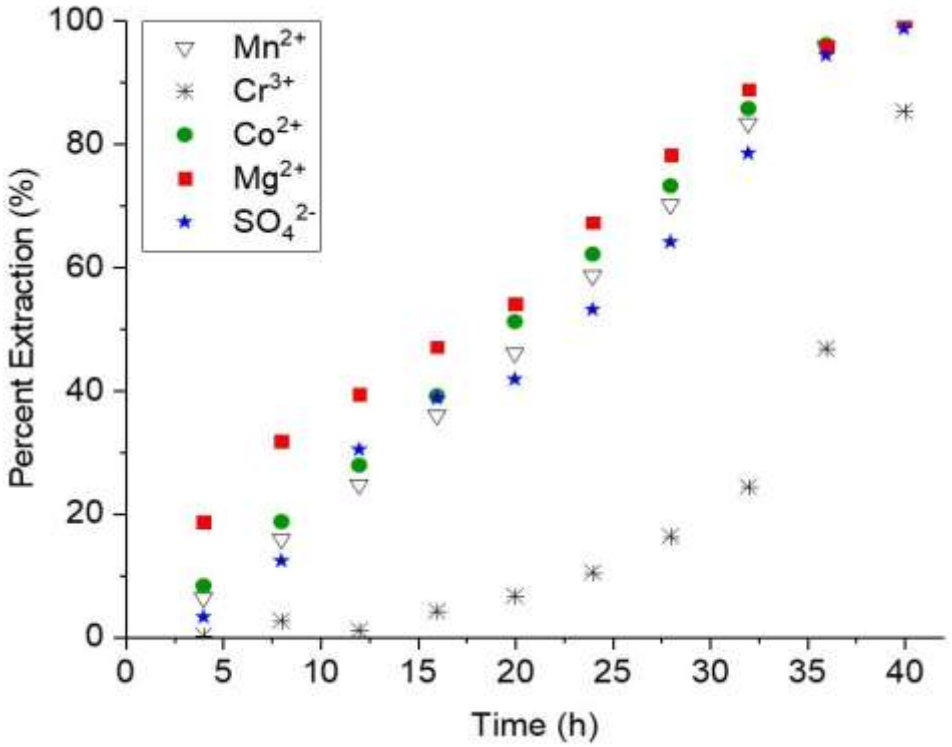

Figure 11 - Percent extraction of the main species during 40h of electrodialysis.

As electrodialysis is conducted, the concentration of these ions in the diluted compartment decreases; hence, the system adjusts itself and starts to transport ions that present lower mobility, to guarantee the electroneutrality principle. Note that after 30h, the bivalent ions achieved values of percent extraction between 70%-80%. Hence, their low concentration in the diluted compartment allowed the intense transfer of Cr^{3+} through the CEM because the competition between bivalent and trivalent ions was not so intense from that moment.

The current efficiency associated with each species in the solution throughout the one-batch electrodialysis was calculated by Equation (3) and the results are shown in Figure 12.

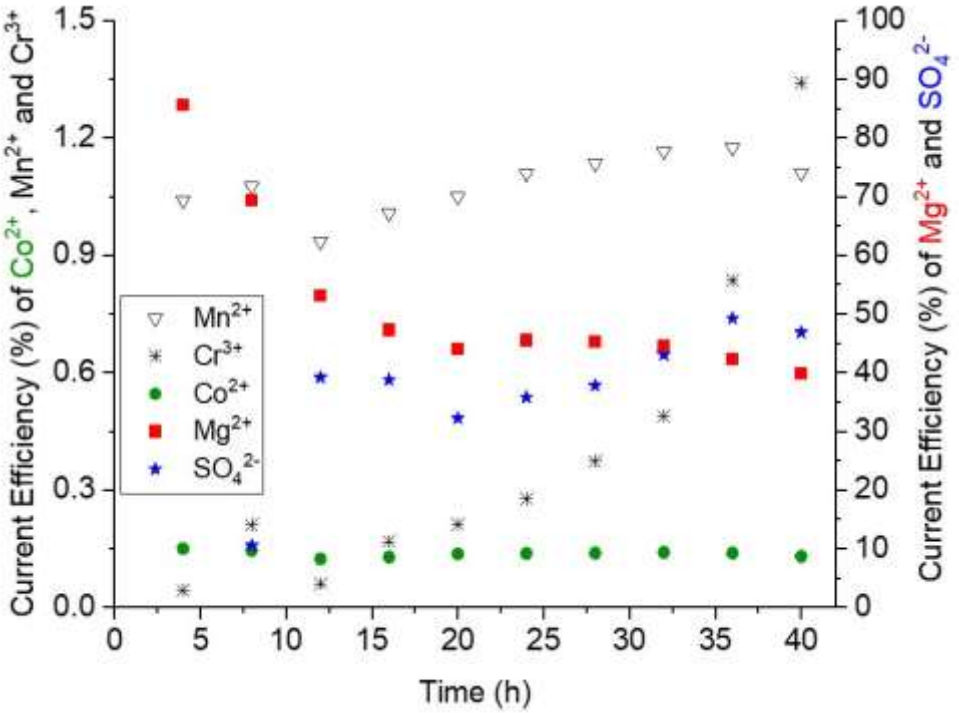

Figure 12 - Current efficiency of the main ionic species during 40h of electrodialysis.

According to Figure 12, the current efficiencies of Mg^{2+} and mainly SO_4^{2-} were considerably greater than the other ions. For magnesium, this may be explained by its greater concentration in solution compared to the other cations (Table 2); hence, it was preferentially transferred through the cation-exchange membrane. For SO_4^{2-} ions, its current efficiency was considerably greater because theoretically, it was the only species that crossed the anion-exchange membrane.

Note that the current efficiency of Co^{2+} ions remained virtually constant throughout the experiment, whereas for Mn^{2+} and Mg^{2+} ions, the current efficiency decreased until 12h and then they also remained constant. In turn, for Cr^{3+} ions, an oscillation was verified until 12h and then it showed a sharp increase, reaching values considerably higher than the other cations. This behavior agrees with the results of percent extraction of both tests (Figure 8 and Figure 11) and percent concentration (Figure 9) since one can see that the transfer of Cr^{3+} ions increased when the concentration of the other cations in the diluted solution decreased. As discussed, this occurred because of the competition between the species, since Cr^{3+} ions presented lower mobility, lower diffusion coefficient, and greater Stokes radius than the other cations. As the solution was acid, protons were also responsible for part of the current efficiency, which explains the values different from 100% considering all the species in Figure 12.

Lastly, the behavior of SO_4^{2-} ions supports our suggestion of water dissociation at the AEM. Note that its current efficiency increased considerably until 12h; then, it decreased and remained virtually constant until the end of the test. Hence, when the concentration of the diluted solution decreased (12h), the limiting current density of the membrane/electrolyte system also decreased, and it started to operate under overlimiting conditions. From that moment, water dissociation was intensified at the AEM, and OH^- ions were intensively transported through it, competing with SO_4^{-2} because hydroxyl ions have lower Stokes radius and greater diffusion coefficient than sulfate ions (Table S1 – Supplementary Material).

Figure 13 shows the energy consumption determined for the main ionic species present in the solution.

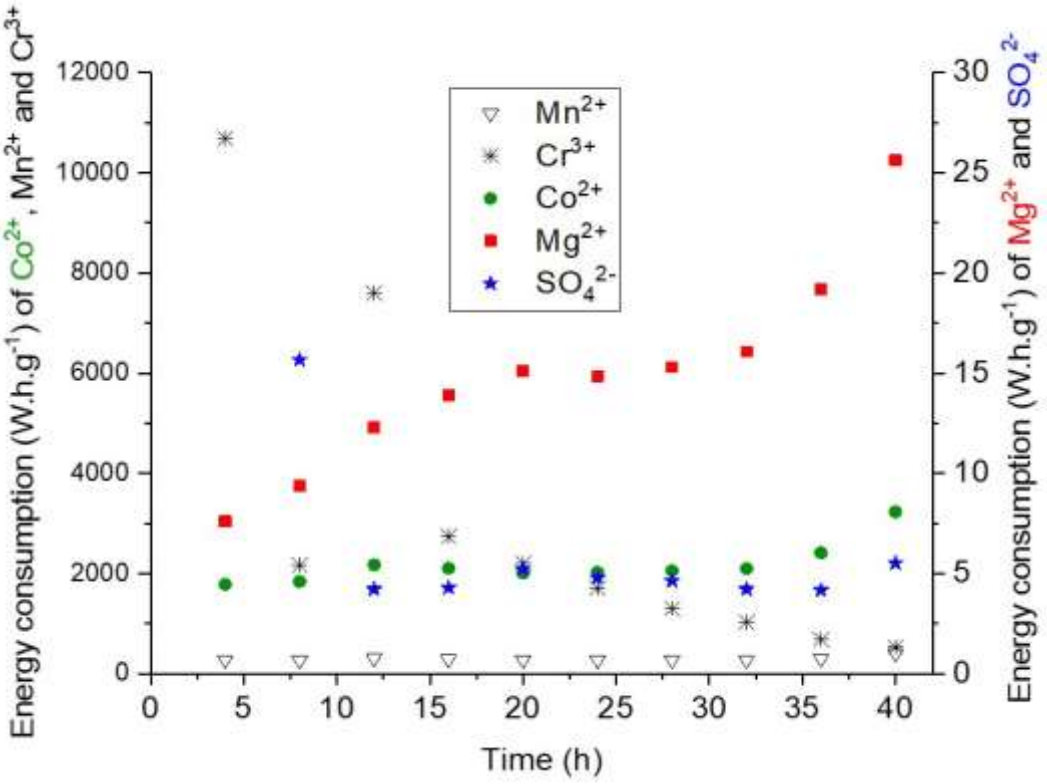

Figure 13 - Energy consumption of the main ionic species during 40h of electrodialysis.

The high values of energy consumption associated with the transfer of Co^{2+} ions can be attributed to its low concentration in the solution, while the inverse behavior was observed for Mg^{2+} and SO_4^{2-} ions due to their high concentration. As shown in Equation (4), energy consumption and the mass of transported species show an inverse proportion. For Cr^{3+} ions, its energy consumption decreased considerably as

electrodialysis was conducted, which confirms that its transfer was intensified throughout the experiment as the other species migrated to the concentrate compartment. Note that the decrease in energy consumption of Cr^{3+} ions was very intense mainly in the first 16 hours, which is the period when the energy consumption of Co^{2+} and Mn^{2+} ions increased before achieving a plateau. The energy consumption of the electrodialysis stack was calculated considering the migration of all ions in the solution through the membranes; in 40 hours of electrodialysis, the energy consumption was 145.2 W.h.

4. Conclusions

The use of electrodialysis as a complementary technique for the recovery of metals from solutions from the nickel laterite processing was evaluated. The solution to be desalted presented magnesium, manganese, cobalt, chromium, and sulfate ions. Three batches were conducted and the test lasted 136 hours. Values of percent extraction above 98% were obtained for Co^{2+}, Mn^{2+}, Mg^{2+}, and SO_4^{2-}. In turn, considerably lower values were obtained for Cr^{3+} ions. The transfer of chromium through the cation-exchange membrane was hindered because of its greater Stokes radius, lower diffusion coefficient, and lower selectivity of the cation-exchange membrane to trivalent ions compared to the other cations in the solution. A variation between the percent extraction and the percent concentration of the main ions in the solution was verified, which may be explained by the transfer of solvent (water) through the membranes due to osmotic and electro-osmotic effects. Such effects should be considered in an eventual scaling-up and may be minimized by adopting multiple stages. The occurrence of water dissociation at the ion-exchange membranes was suggested by the evaluation of solution pH throughout the experiment and SEM/EDS analysis.

An electrodialysis test was also conducted in a single batch to evaluate the percent extraction at several moments of the experiment, in addition to the current efficiency and energy consumption associated with each species in solution. The results confirmed the competition between chromium and the other cations for crossing the cation-exchange membrane; Cr^{3+} ions began to be intensively transported when the concentration of the other species decreased in the diluted compartment. The results from the one-batch electrodialysis also suggested the occurrence of water dissociation at the anion-exchange membrane.

Electrodialysis showed to be a promising technique for extracting metals from a solution from nickel laterite processing and concentrating them for further purification. The values of percent concentration obtained for the metals were 178% for Co^{2+}, 145% for Mn^{2+}, 164% for Mg^{2+}, and 79% for Cr^{3+}. The diluted solutions obtained at the end of the tests may be reused in the process, whereas the concentrated one can be forwarded to subsequent steps for purifying the metals.

Acknowledgments

The authors gratefully acknowledge the financial support given by funding agencies CNPq (Process 141346/2016-7; 171241/2017-7; 160320/2019-4) and FAPESP (Process 2012/51871-9). This study was financed in part by the Coordenação de Aperfeiçoamento de Pessoal de Nível Superior - Brasil (CAPES) - Finance Code 001 (Processes 88881.190502/2018-01 and 88887.362657/2019-00).

References

[1] T. Norgate, S. Jahanshahi, Assessing the energy and greenhouse gas footprints of nickel laterite processing, Miner. Eng. 24 (2011) 698–707. doi:10.1016/j.mineng.2010.10.002.

[2] G.M. Mudd, Z. Weng, S.M. Jowitt, I.D. Turnbull, T.E. Graedel, Quantifying the recoverable resources of by-product metals: The case of cobalt, Ore Geol. Rev. 55 (2013) 87–98. doi:10.1016/j.oregeorev.2013.04.010.

[3] P. Fröhlich, T. Lorenz, G. Martin, B. Brett, M. Bertau, World Mineral Production, Angew. Chemie - Int. Ed. 56 (2017) 2544–2580. doi:10.1002/anie.201605417.

[4] A. Oxley, N. Barcza, Hydro-pyro integration in the processing of nickel laterites, Miner. Eng. 54 (2013) 2–13. doi:10.1016/j.mineng.2013.02.012.

[5] S. Kursunoglu, Z.T. Ichlas, M. Kaya, Solvent extraction process for the recovery of nickel and cobalt from Caldag laterite leach solution: The first bench scale study, Hydrometallurgy. 169 (2017) 135–141.

530 doi:10.1016/j.hydromet.2017.01.001.

531 [6] T.Z. Sadyrbaeva, Separation of cobalt(II) from nickel(II) by a hybrid liquid
532 membrane-electrodialysis process using anion exchange carriers, Desalination.
533 365 (2015) 167–175. doi:10.1016/j.desal.2015.02.036.

534 [7] J. Rydberg, M. Cox, C. Musikas, G.R. Choppin, Solvent Extraction Principles
535 and Practice, Revised and Expanded, Taylor & Francis, 2004.
536 doi:10.1201/9780203021460.

537 [8] K.G. Fisher, Cobalt Processing Developments, in: South. African Inst. Min.
538 Metall. - 6th South. African Base Met. Conf., 2011: pp. 237–258.

539 [9] D.L. Jones, T.M. McCoy, K.E. Mayhew, C.Y. Cheng, K.R. Barnard, W. Zhang,
540 A New Process for Cobalt – Nickel Separation, in: ALTA Metall. Serv., 2010: p.
541 19.

542 [10] P. Aliprandini, M.M. Jiménez Correa, J.A. Soares Tenório, D.C.R. Espinosa,
543 Influence of Metallic Impurities on Solvent Extraction of Cobalt and Nickel from
544 a Laterite Waste Liquor, in: REWAS 2019, Miner. Mater. Ser., 2019: pp. 137–
545 142. doi:10.1007/978-3-030-10386-6_16.

546 [11] F.K. Crundwell, M.S. Moats, V. Ramachandran, T.G. Robinson, W.G.
547 Davenport, Extractive metallurgy of nickel, cobalt and platinum-group metals,
548 Elsevier Ltd., 2011.

549 [12] P. Aliprandini, M.M.J. Correa, J.A.S. Tenório, D.C.R. Espinosa, The Effect of
550 Extractant Mixture During Solvent Extraction of Cobalt, 56th Annu. Conf.
551 Metall. (2017) 8.

552 [13] T. Scarazzato, Z. Panossian, J.A.S. Tenório, V. Pérez-Herranz, D.C.R. Espinosa,
553 Water reclamation and chemicals recovery from a novel cyanide-free copper
554 plating bath using electrodialysis membrane process, Desalination. 436 (2018)
555 114–124. doi:10.1016/j.desal.2018.01.005.

556 [14] K.S. Barros, T. Scarazzato, V. Pérez-Herranz, D.C.R. Espinosa, Treatment of
557 Cyanide-Free Wastewater from Brass Electrodeposition with EDTA by

Electrodialysis: Evaluation of Underlimiting and Overlimiting Operations, Membranes (Basel). 10 (2020) 69. doi:10.3390/membranes10040069.

[15] M. Paidar, V. Fateev, K. Bouzek, Membrane electrolysis—History, current status and perspective, Electrochim. Acta. 209 (2016) 737–756. doi:10.1016/j.electacta.2016.05.209.

[16] N.D. Pismenskaya, V. V. Nikonenko, V.I. Zabolotsky, R. Sandoux, G. Pourcelly, A.A. Tskhay, Effects of the desalination chamber design on the mass-transfer characteristics of electrodialysis apparatuses at overlimiting current densities, Russ. J. Electrochem. 44 (2008) 818–827. doi:10.1134/S1023193508070082.

[17] L. Bazinet, T.R. Geoffroy, Electrodialytic processes: Market overview, membrane phenomena, recent developments and sustainable strategies, Membranes (Basel). 10 (2020) 1–72. doi:10.3390/membranes10090221.

[18] K.S. Barros, M.C. Martí-Calatayud, E.M. Ortega, V. Pérez-Herranz, D.C.R. Espinosa, Chronopotentiometric study on the simultaneous transport of EDTA ionic species and hydroxyl ions through an anion-exchange membrane for electrodialysis applications, J. Electroanal. Chem. 879 (2020) 114782. doi:10.1016/j.jelechem.2020.114782.

[19] K.S. Barros, M.C. Martí-Calatayud, T. Scarazzato, A.M. Bernardes, D.C.R. Espinosa, V. Pérez-Herranz, Investigation of ion-exchange membranes by means of chronopotentiometry: A comprehensive review on this highly informative and multipurpose technique, Adv. Colloid Interface Sci. 293 (2021) 102439. doi:10.1016/j.cis.2021.102439.

[20] K.S. Barros, M.C. Martí-Calatayud, V. Pérez-Herranz, D.C.R. Espinosa, A three-stage chemical cleaning of ion-exchange membranes used in the treatment by electrodialysis of wastewaters generated in brass electroplating industries, Desalination. 492 (2020) 114628. doi:10.1016/j.desal.2020.114628.

[21] K.S. Barros, T. Scarazzato, D.C.R. Espinosa, Evaluation of the effect of the solution concentration and membrane morphology on the transport properties of Cu(II) through two monopolar cation–exchange membranes, Sep. Purif. Technol. 193 (2018) 184–192. doi:10.1016/j.seppur.2017.10.067.

588 [22] R. Valerdi-Pérez, J. Ibáez-Mengual, Current-voltage curves for an electrodialysis
589 reversal pilot plant: Determination of limiting currents, Desalination. 141 (2001)
590 23–37. doi:10.1016/S0011-9164(01)00386-1.

591 [23] J.J. Krol, M. Wessling, H. Strathmann, Concentration polarization with
592 monopolar ion exchange membranes: Current-voltage curves and water
593 dissociation, J. Memb. Sci. 162 (1999) 145–154. doi:10.1016/S0376-
594 7388(99)00133-7.

595 [24] T. Scarazzato, D.C. Buzzi, A.M. Bernardes, D.C.R. Espinosa, Current-Voltage
596 Curves for Treating Effluent Containing Hedp : Determination of the Limiting
597 Current, Brazilian J. Chem. Eng. 32 (2015) 831–836.

598 [25] I. Puigdomench, Hydra Medusa — Make Equilibrium Diagrams using
599 Sophisticated Algorithms, (2001).

600 [26] K.S. Barros, D.C.R. Espinosa, Chronopotentiometry of an anion-exchange
601 membrane for treating a synthesized free-cyanide effluent from brass
602 electrodeposition with EDTA as chelating agent, Sep. Purif. Technol. 201 (2018)
603 244–255. doi:10.1016/j.seppur.2018.03.013.

604 [27] T. Scarazzato, Z. Panossian, M. García-Gabaldón, E.M. Ortega, J.A.S. Tenório,
605 V. Pérez-Herranz, D.C.R. Espinosa, Evaluation of the transport properties of
606 copper ions through a heterogeneous ion-exchange membrane in etidronic acid
607 solutions by chronopotentiometry, J. Memb. Sci. 535 (2017) 268–278.
608 doi:10.1016/j.memsci.2017.04.048.

609 [28] M.C. Martí-Calatayud, D.C. Buzzi, M. García-Gabaldón, E. Ortega, A.M.
610 Bernardes, J.A.S. Tenório, V. Pérez-Herranz, Sulfuric acid recovery from acid
611 mine drainage by means of electrodialysis, Desalination. 343 (2014) 120–127.
612 doi:10.1016/j.desal.2013.11.031.

613 [29] E.R. Nightingale, Phenomenological Theory of Ion Solvation. Effective Radii of
614 Hydrated Ions, J. Phys. Chem. 63 (1959) 1381–1387. doi:10.1021/j150579a011.

615 [30] W.M. Haynes, CRC Handbook of Chemistry and Physics, 97th Edition, CRC
616 Press, 2016.

[31] M.C. Martí-Calatayud, M. García-Gabaldón, V. Pérez-Herranz, E. Ortega, Determination of transport properties of Ni(II) through a Nafion cation-exchange membrane in chromic acid solutions, J. Memb. Sci. 379 (2011) 449–458. doi:10.1016/j.memsci.2011.06.014.

[32] V. V. Nikonenko, A. V. Kovalenko, M.K. Urtenov, N.D. Pismenskaya, J. Han, P. Sistat, G. Pourcelly, Desalination at overlimiting currents: State-of-the-art and perspectives, Desalination. 342 (2014) 85–106. doi:10.1016/j.desal.2014.01.008.

[33] S. Logette, C. Eysseric, G. Pourcelly, A. Lindheimer, C. Gavach, Selective permeability of a perfluorosulphonic membrane to different valency cations. Ion-exchange isotherms and kinetic aspects, J. Memb. Sci. 144 (1998) 259–274. doi:10.1016/S0376-7388(98)00062-3.

[34] A. Chapotot, G. Pourcelly, C. Gavach, Transport competition between monovalent and divalent cations through cation-exchange membranes. Exchange isotherms and kinetic concepts, J. Memb. Sci. 96 (1994) 167–181. doi:10.1016/0376-7388(94)00107-3.

[35] M.C. Martí-Calatayud, D.C. Buzzi, M. García-Gabaldón, A.M. Bernardes, J.A.S. Tenório, V. Pérez-Herranz, Ion transport through homogeneous and heterogeneous ion-exchange membranes in single salt and multicomponent electrolyte solutions, J. Memb. Sci. 466 (2014) 45–57. doi:10.1016/j.memsci.2014.04.033.

[36] M. Taky, G. Pourcelly, C. Gavach, A. Elmidaoui, Chronopotentiometric response of a cation exchange membrane in contact with chromiumIII solutions, Desalination. 105 (1996) 219–228. doi:10.1016/0011-9164(96)00079-3.

[37] R.F. Dalla Costa, J.Z. Ferreira, C. Deslouis, Electrochemical study of the interactions between trivalent chromium ions and Nafion® perfluorosulfonated membranes, J. Memb. Sci. 215 (2003) 115–128. doi:10.1016/S0376-7388(02)00607-5.

[38] H. Strathmann, Chapter 6 Ion-Exchange Membrane Processes in Water Treatment, Elsevier, 2010. doi:10.1016/S1871-2711(09)00206-2.

[39] V.K. Indusekhar, N. Krishnaswamy, Water transport studies on interpolymer ion-exchange membranes, Desalination. 52 (1985) 309–316. doi:10.1016/0011-9164(85)80040-0.

[40] N. Lakshminarayaniah, Electro-osmotic permeability of ion-exchange resin membranes, Proc. Indian Acad. Sci. - Sect. A. 55 (1962) 200–212. doi:10.1007/BF03048976.

[41] L.P. Ling, H.F. Leow, M.R. Sarmidi, Citric acid concentration by electrodialysis: Ion and water transport modelling, J. Memb. Sci. 199 (2002) 59–67. doi:10.1016/S0376-7388(01)00678-0.